Electron heating in the conduction band of insulators irradiated by ultrashort laser pulses

H. Bachau,[1] A. N. Belsky,[1] P. Martin,[1] A. N. Vasil'ev,[2,*] and B. N. Yatsenko[1,3]
[1]*Centre des Lasers Intenses et Applications, UMR5107 CNRS-Université de Bordeaux I-CEA, Université de Bordeaux I, 33405 Talence Cedex, France*
[2]*Physics Department, Moscow State University, Vorob'evy Gory, Moscow 119992, Russia*
[3]*Scobeltsyn Institute of Nuclear Physics, Moscow State University, Vorob'evy Gory, Moscow 119992, Russia*
(Received 3 April 2006; revised manuscript received 1 November 2006; published 26 December 2006)

We investigate the theoretical problem of electron heating in the conduction band of wide band gap insulators and semiconductors induced by intense femto-second Ti:Sapphire laser pulses. We analyze in detail the heating mechanism due to the sequence of direct interbranch transitions in the conduction band, which has been shown to be of crucial importance in previous work. This analysis is fulfilled by resolving the time dependant Schrödinger equation (TDSE) in a basis of Bloch functions for the CsI crystal. The field is represented semiclassically and the laser-electron interaction is treated in the dipole approximation. The presented approaches are based on a one-active electron approximation. First the TDSE is solved in a basis of Bloch functions, in one dimension, the influence of laser and crystal parameters on the electron spectra is studied. The electron transfer from the lower conduction band to the higher one is already effective at intensity of 3×10^{12} W/cm^2. Then the problem is solved in three dimension. The electron spectra is consistent with the experimental results, we note in particular the presence of a large plateau at intensities of the order of the terawatt per square centimeter.

DOI: 10.1103/PhysRevB.74.235215 PACS number(s): 42.50.Hz, 61.80.Ba, 79.60.−i

I. INTRODUCTION

The interaction of ultrashort high intensity laser pulses with transparent (wide band gap) solids involves a large number of elementary processes. Recent experiments, accompanied by theoretical models,[1–4] show that direct interband transitions in the conduction band play an essential role in the electron heating resulting from the interaction of wide band-gap insulators with short IR femtosecond laser pulses. The cascade of these processes leads to the creation of electrons with unexpectedly high energies. From our estimations, the microscopic processes (like electron-photon-phonon heating, electron-phonon relaxation, inelastic electron-electron scattering, Auger processes, etc.) cannot explain the production of high energy electrons.[2] Note that the low energy electrons cannot be observed in the experiments due to the crystal affinity and for experimental reasons. We showed that, for example, in CsI irradiated by a Ti:Sapphire laser radiation at 3 TW/cm^2 (1 TW$=10^{12}$ W), the electron spectrum shows a wide plateau with a cutoff at 24 eV (Ref. 1) (it is about a hundred times the ponderomotive potential U_p). Under similar conditions a plateau with a cutoff at 10 U_p is expected in the atomic case.[5] Whereas the large variety of microscopic processes (cited above) occurring in insulators after a weak optical excitation has been extensively studied, all these processes remain poorly understood at the regime of intense optical excitation. It is in particular the case of the mechanism of heating due to the cascade of one- and multiphoton interbranch transitions in the conduction band of insulators, although its importance has been already emphasized.[6] Elementary processes are interconnected; moreover the supposition of successive and independent processes is violated since the typical mean time between two processes is smaller than their typical duration.

Electron heating in the conduction band of wide band-gap insulators and semiconductors occurs when an electron in the conduction band scatters on the crystal lattice, absorbs one or more photons and populates the upper branch of the conduction band. Such sequence of processes occurs during the pulse duration, thus, it leads to an effective heating mechanism.

The theoretical description of such transition cascades is rather complicated. The interbranch transition rate was calculated in previous works.[2,3,7] It was shown that, for a large variety of wide band-gap crystals, the transition rate associated to two- and three-photon transitions becomes comparable with one-photon transition rates at intensities of several TW/cm^2. On the basis of these calculations we proposed a model of cascade transitions, which qualitatively explains the spectra of electrons in the conduction band. The simplified form of this cascade model (without emission of photons) was also subsequently applied to treat the case of impact ionization in wide band-gap insulators.[8] However, this simple model has some drawbacks. First, resonant transitions (i.e., the situation where the difference ΔE between energy levels equals the photon energy $\hbar\omega$) are presumed to exist in this model, i.e., each electron can absorb (or emit) a photon and transfer to the higher (lower) level at any time. This, obviously, leads to an overestimation of the heating efficiency. Second, the model used to represent the band structure is not realistic, in particular, the density of states in the conduction band should decrease with the electron energy as $\sim\varepsilon^{-1/2}$ in the one-dimensional case (1D) or increase as $\sim\varepsilon^{1/2}$ in the three-dimensional case (3D), but it is supposed to be constant in the cascade model.[2,3,7,8] Third, this simple model does not account for the transitions through the virtual states. In our approach we overcome these problems by using a model where the TDSE is resolved in a basis of Bloch functions[1,4] calculated in a realistic potential. This model can efficiently describe the mechanism of electron heating by intense laser pulses; it has been previously used to treat high-order harmonic generation in a crystalline solid.[9] The under-

standing of the heating mechanism is of particular importance for the description of electronic excitation dynamics in conduction band of insulators at excitation intensities close to the optical breakdown threshold. Detailed study of this electron heating mechanism is also needed to improve the radiation resistance of optical materials.

In the following section we present the theoretical approach. First we resolve the stationary problem, by using Bloch functions and a pseudopotential to describe the electronic states in the conduction band. The heating mechanism is treated as a two-step mechanism; one-photon absorption from a defect state to the lower conduction branch followed by the electron heating within the conduction band. The first step is in fact treated in a phenomenological manner, as one-photon absorption from a defect state to the lower conduction band. Then the TDSE is resolved in the basis of the Bloch functions representing the conduction band. In Secs. III and IV the problem is resolved in 1D and 3D, respectively. The main features of the photoelectron spectra are shown; the influence of laser crystal parameters is discussed in this context.

II. THEORY

First we consider the free-field (i.e., without the laser field) stationary problem for an electron in the conduction band of an insulator. The stationary electronic levels are determined by using the time-independent Schrödinger equation for an electron of wave-vector $\mathbf{k}$, which is written:

$$\hat{H}_c(\mathbf{r})\theta_{\mathbf{k}}^n(\mathbf{r}) = E_{\mathbf{k}}^n \theta_{\mathbf{k}}^n(\mathbf{r}), \tag{2.1}$$

where $\theta_{\mathbf{k}}^n(\mathbf{r})$ is the one-electron Bloch wave function with a wave-vector $\mathbf{k}$, n is the index of the branch. In the simplest approach the free-field crystal Hamiltonian can be written as $\hat{H}_c(\mathbf{r}) = \hat{H}_f(\mathbf{r}) + U(\mathbf{r})$, where $\hat{H}_f(\mathbf{r}) = -\frac{\hbar^2}{2m}\boldsymbol{\nabla}^2$ is the Hamiltonian for a free electron, $U(\mathbf{r})$ is a periodical crystal potential, which can be represented, for example, by using the theory of pseudopotentials (see, for example, Refs. 9–13), and m is the free electron mass. Since the potential energy is periodical, it is represented by a Fourier series:

$$U(\mathbf{r}) = \sum_{\mathbf{G}} U_{\mathbf{G}} \exp(i\mathbf{G}\cdot\mathbf{r}), \tag{2.2}$$

where $\mathbf{G} = \Sigma_{\alpha=1}^{3} m_\alpha \mathbf{b}_\alpha$ are the reciprocal lattice vectors, while m_α are integers and $\mathbf{b}_\alpha$ are the primitive vectors of the reciprocal crystal lattice. For crystals with simple cubic lattice $\mathbf{b}_\alpha$ compose a set of orthogonal vectors with length $b_\alpha = 2\pi/a$, where a is the lattice period. Here

$$U_{\mathbf{G}} = \frac{1}{\nu_c}\int_{\nu_c} \exp(-i\mathbf{G}\cdot\mathbf{r})U(\mathbf{r})d\mathbf{r},$$

where ν_c is the volume of an elementary cell. Since the zero level of the potential energy can be arbitrarily chosen, we set $U_{\mathbf{G}=0} = 0$. For the case of crystals, which has a center of inversion, Fourier components associated to symmetrical lattice vectors are equal; $U_{-\mathbf{G}} = U_{\mathbf{G}}$.

Equation (2.1) can be resolved for each value of wave-vector $\mathbf{k}$, by expanding the solution over a plane wave basis set:

$$\theta_{\mathbf{k}}^n(\mathbf{r}) = \sum_{j=1}^{N_{\max}} C_{\mathbf{k},j}^n \exp[i(\mathbf{k}+\mathbf{G}_j)\mathbf{r}], \tag{2.3}$$

where $N_{\max}$ is the number of plane waves used in the basis.

Introducing the expansion (2.3) in Eq. (2.1), we obtain an eigenvalue system, which is solved using standard routines. Finally, one obtains the eigenfunctions $\theta_{\mathbf{k}}^n(\mathbf{r})$ and eigenenergies $E_{\mathbf{k}}^n$ for the stationary problem. The number of solutions of the stationary problem (i.e., the number of branches in the Brillouin zone) is $N_{\max}$, given in Eq. (2.3). The eigenenergies $E_{\mathbf{k}}^n$ represent the structure of the energy bands while the eigenfunctions are used to calculate the dipole matrix elements. Once the eigenenergies $E_{\mathbf{k}}^n$ and dipole matrix elements have been determined, the dynamical part of the problem is investigated, the approach is described below.

The dynamics of an electron in the conduction band of an insulator under laser irradiation is described by the time dependent Schrödinger equation (TDSE). In this approach, the wave function $\psi(\mathbf{r},t)$ of an electron in the conduction band is written:

$$i\hbar\frac{\partial\psi_{\mathbf{k}}(\mathbf{r},t)}{\partial t} = \hat{H}(\mathbf{r},t)\psi_{\mathbf{k}}(\mathbf{r},t). \tag{2.4}$$

The Hamiltonian of the nonstationary problem is given by the following expression:

$$\hat{H}(\mathbf{r},t) = \hat{H}_c(\mathbf{r}) + \hat{H}_{\text{int}}(t), \tag{2.5}$$

where $\hat{H}_c(r)$ is the crystal Hamiltonian [see Eq. (2.1)] and $\hat{H}_{\text{int}}(t)$ is the laser-electron interaction Hamiltonian. Within the dipole approximation $\hat{H}_{\text{int}}(t)$ is given by (in the Coulomb gauge):

$$H_{\text{int}}(t) = \frac{e}{mc}\mathbf{A}(t)\cdot\hat{\mathbf{p}}, \tag{2.6}$$

where e is the absolute value of electron charge, c is the light velocity, $\hat{\mathbf{p}} = -i\hbar\frac{\partial}{\partial\mathbf{r}}$ is the momentum operator, $\mathbf{A}(t)$ is the time-dependant vector potential.

For the calculations considered in this paper, the vector potential has been taken in the following form:

$$\mathbf{A}(t) = \mathbf{e}_f A_0\left(\cos\frac{\pi t}{T}\right)^2 \cos\omega t, \quad -T/2 \leqslant t \leqslant T/2, \tag{2.7}$$

and $\mathbf{A}(t) = 0$ for $|t| > T/2$. $\mathbf{e}_f$ is the polarization unit vector, ω is the laser frequency, T is the pulse duration, and $A_0 = cE_0/\omega$, where $E_0 = \sqrt{\frac{8\pi I_0}{cn_0}}$ is the electric field amplitude, c is the light velocity, n_0 is the refractive index of the crystal, and I_0 is the peak laser intensity. The electric field value of $E_0 = 1$ a.u. corresponds to an intensity of 3.51×10^{16} W/cm^2 (for $n_0 = 1$).

We assume that the dynamics of electronic excitations in an insulator under laser irradiation can be divided into two

stages; the ionization stage (which includes the ionization of defects and eventually the multiphoton ionization from the valence band) and the stage of electron heating in the conduction band. It is worth to recall that it is the first stage which defines the initial condition (i.e., the population of lower conduction bands) subsequently used in the TDSE. We assume that laser intensities are such that one-photon ionization from defects dominates over multiphoton ionization from the valence band. Therefore, in our approximation, only the lower branch of the conduction band is populated at the beginning of the second stage. Thus, the initial condition for Eq. (2.4) has the following form:

$$\psi_{\mathbf{k}}(\mathbf{r}, t = -T/2) = \theta^1_{\mathbf{k}}(\mathbf{r}), \tag{2.8}$$

where $\theta^1_{\mathbf{k}}(\mathbf{r})$ is the wave function of the stationary problem corresponding to the lowest branch of the conduction band ($E^1_{\mathbf{k}} < E^n_{\mathbf{k}}$, $\forall n = 2 \cdots N_{\max}$, $\forall \mathbf{k}$). This supposition for initial conditions can be restricted by the proposition that only a region in the Brillouin zone is populated. In this case only equations with $\mathbf{k}$ corresponding to populated states are involved in the set (2.4).

The general solution of Eq. (2.4) is written:

$$\psi_{\mathbf{k}}(\mathbf{r}, t) = \sum_{m=1}^{N_{\max}} \alpha^m_{\mathbf{k}}(t)\, \theta^m_{\mathbf{k}}(\mathbf{r}). \tag{2.9}$$

Since $\langle \theta^i_{\mathbf{k}}(\mathbf{r}) | \theta^j_{\mathbf{k}}(\mathbf{r}) \rangle = \delta_{ij}$, where δ_{ij} is a Kronecker delta function, the time-dependant coefficients $\alpha^m_{\mathbf{k}}(t)$ are evaluated by solving the following system of equations:

$$i\hbar \frac{\partial \alpha^q_{\mathbf{k}}(t)}{\partial t} = E^q_{\mathbf{k}} \alpha^q_{\mathbf{k}}(t) + \frac{e}{mc} \mathbf{A}(t) \sum_{m=1}^{N_{\max}} \mathbf{p}^{qm}_{\mathbf{k}} \alpha^m_{\mathbf{k}}(t), \quad q = 1 \cdots N_{\max},$$

$$\alpha^1_{\mathbf{k}}(t = -T/2) = 1,$$

$$\alpha^p_{\mathbf{k}}(t = -T/2) = 0, \quad p = 2 \cdots N_{\max}, \tag{2.10}$$

where $\mathbf{p}^{qm}_{\mathbf{k}} = \langle \theta^q_{\mathbf{k}}(\mathbf{r}) | \hat{\mathbf{p}} | \theta^m_{\mathbf{k}}(\mathbf{r}) \rangle$ are dipole matrix elements.

From the above equations, it is clear that only direct interband electron transitions are taken into account; the electron wave vector does not change, therefore our approach takes into account only transitions due to the interaction with the laser field; effects like electron-phonon scattering, which involve different wave vectors, and inelastic electron-electron scattering, which, moreover leads to the change of the number of active electrons, are neglected. Therefore one has to solve Eqs. (2.4)–(2.10) for each value of $\mathbf{k}$. Thus, supposing that initially (i.e., at the beginning of the second stage) an electron with a wave-vector $\mathbf{k}$ exists in the conduction band with a probability equal to 1, one obtains the following expression for the probability that the electron will be on the band m of the conduction band after the interaction with the laser pulse:

$$P^m_{\mathbf{k}} = |\alpha^m_{\mathbf{k}}(t = T/2)|^2, \tag{2.11}$$

with $\Sigma_{m=1}^{N_{\max}} P^m_{\mathbf{k}} = 1$. Thus, provided we know the initial wave-vector distribution $f(k)$ of the electrons [or electron energy distribution $f(E)$], the final spectrum of electrons in the conduction band can be obtained.

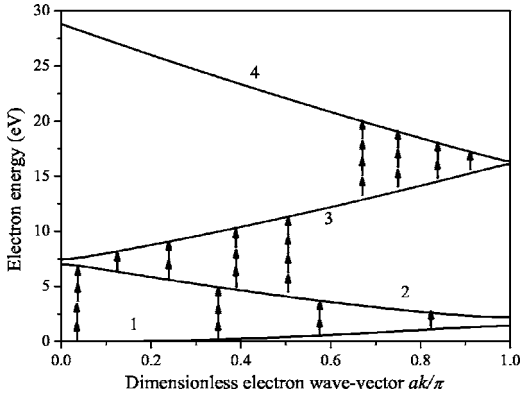

FIG. 1. The conduction band structure in the first Brillouin zone for the one-dimensional case and a nearly free electron model (lattice constant and U_g correspond to CsI crystal). One-, two-, three-, and four-photon ($\hbar\omega = 1.55$ eV) transitions are marked out by arrows.

III. RESOLUTION OF THE TDSE IN ONE DIMENSION

First we simplify the problem by considering a one-dimensional (1D) space for the wave vector.[1] Though this model is rather crude, it allows us to get an insight into the dominant physical processes. Thus, as we will see below, it is of great help to analyze the results in 3D. We have noticed in Sec. II that the probability distribution P^m_k depends on the following parameters: the peak laser intensity I_0, the photon energy $\hbar\omega$, the pulse duration T, and crystal parameters (the Fourier components $U_{\mathbf{G}}$ and the lattice period a). For the CsI crystal, the lattice period is $a = 4.57$ Å. In the present one-dimensional simulation we have considered the following model for the Fourier component U_G: $U_{-G} = U_G$, $U_{G=0} = 0$, $U_{G=2n\pi/a} = n^{-1} U_{G=2\pi/a}$ [note that Kronig-Penny model where the potential is treated as a stepwise well of width b and depth U_0 results in

$$U_{G=2n\pi/a} = U_0 \sin\left(\frac{\pi b n}{a}\right) \Big/ \pi n$$

with typical n^{-1} asymptotic behavior]. Here we use $U_{G=2\pi/a} = U_g = 0.015$ a.u. $= 0.408$ eV. Figure 1 shows the four lowest branches of the conduction band and the one-, two-, three-, and four-photon transitions in monochromatic electromagnetic field. We see in the figure that interbranch transitions only occur at particular values of the wave-vector $\mathbf{k}$.

Note that the above considerations are valid in the context where the perturbation applies, they do not take into account alternative current (ac) Stark shifts or other high intensity effects; we will return to this point later. Moreover, the density of states in the one-dimensional case behaves like $\varepsilon^{-1/2}$ for high electron energy values ε (compared to $\varepsilon^{1/2}$ in the 3D case). Thus, the photoexcitation of higher states is more difficult in the 1D model; the heating efficiency should be underestimated in this model. In order to have a better understanding of the contribution of one- and multiphoton transitions in the heating process, we study in the following the dependence of P^m_k on the different parameters of the model.

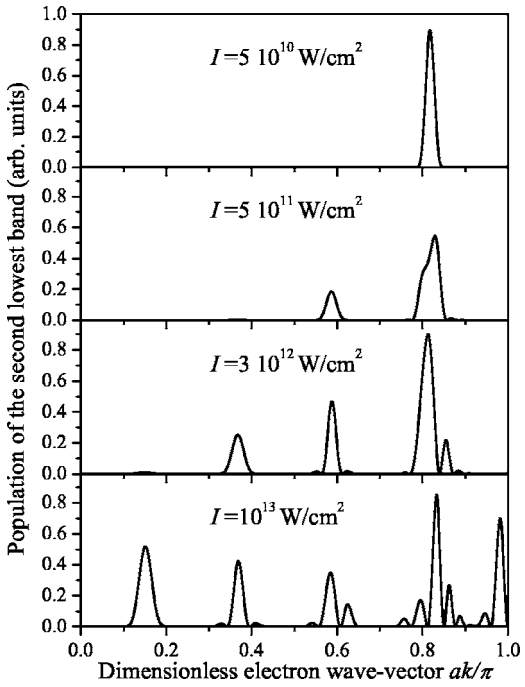

FIG. 2. Dependence of the population of the second lowest band (probability of multi-photon transitions) after the interaction versus the wave-vector (lattice constant and U_g correspond to CsI crystal), for excitation intensities of 0.05 TW/cm^2, 0.5 TW/cm^2, 3 TW/cm^2, and 10 TW/cm^2 and for a pulse duration of T=40 fs, the photon energy is $\hbar\omega$=1.55 eV.

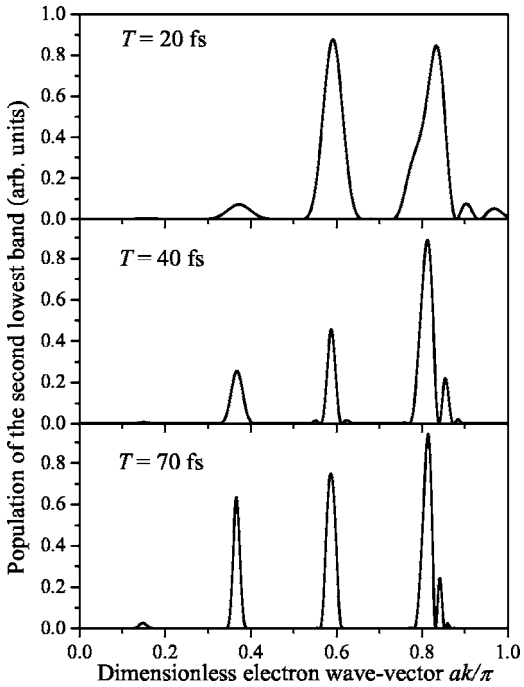

FIG. 3. Dependence of the population of the second lowest band (probability of direct multiphoton transitions) after the interaction versus the wave vector (lattice constant and U_g correspond to CsI crystal), for pulse durations of 20 fs, 40 fs, and 70 fs. The peak laser intensity is I_0=3 TW/cm^2 and the photon energy is $\hbar\omega$ =1.55 eV.

We choose the following default laser pulse parameters: peak laser intensity I_0=3 TW/cm^2; pulse duration T=40 fs, photon energy $\hbar\omega$=1.55 eV, thus the number of cycles in a pulse is about $N\approx 15$. These parameters correspond to experiments recently performed at CELIA.[1–4] We used up to $N_{\max}$=5 plane waves in Eq. (2.3). First we focus on the populations of the first and the second branches, which dominate over the upper branch populations. In our model only the lowest branch is populated at the beginning of the second stage. So, $P_k^1(t=-T/2)=1, \forall k$, while $P_k^2(t=-T/2)=0, \forall k$. Thus, the value $P(k)=P_k^2(t=+T/2)$ is equal to the probability of transition to the upper level for an electron after the interaction with the laser pulse. Figures 2 and 3 show the dependence of the excitation probability $P(k)$ on the laser intensity and pulse duration, respectively.

We have performed calculations by varying the peak intensities from 10^4 W/cm^2 to 10^{13} W/cm^2. Interbranch transitions (due to either one-photon or multiphoton transitions) are not efficient at laser intensities smaller than 10^{10} W/cm^2. At laser intensities close to 3×10^{10} W/cm^2 one-photon transitions start to play a role. As the intensity increases, transitions involving two, three, and four photons appear. The result of these calculations is presented in Fig. 2 for intensities varying from 5×10^{10} W/cm^2 to 10^{13} W/cm^2. One-, two-, three-, and four-photon transitions (cf. Fig. 1) become apparent at different points of the wave-vector space k_n, corresponding to the resonance condition $\Delta E(k_n)=E^2(k)$-$E^1(k)=n\hbar\omega$. Here, k_n corresponds to "primary" peaks and n is the peak order. We introduce a "threshold" I_n for n-photon transition intensity as the intensity at which the second branch population exceeds 0.5 (as a matter of fact this threshold depends on the crystal and on the laser wavelength, which is supposed to be fixed here). Thus, we find $I_1\sim5\times10^{10}$ W/cm^2, $I_2\sim10^{12}$ W/cm^2, $I_3\sim5\times10^{12}$ W/cm^2, and $I_4\sim10^{13}$ W/cm^2. At laser intensities $I\geqslant10^{11}$ W/cm^2 the main peak (at the position k_1) starts to shift and other substructures appear on its right side. This is due to ac Stark shift, which depends linearly on the intensity; its effect is to increase the gap between the branches 1 and 2 at the edge of the Brillouin zone. One-photon resonances appear at different positions of the wave-vector k during the raise and fall of the pulse intensity. Besides the ac Stark shift effects, which also appear for k_2, k_3, and k_4 at higher intensities, interbranch Rabi oscillations occur at high intensity. This explains that the peak height and positions vary with the pulse duration in Fig. 3. Therefore, at high intensity, the dynamics of the populations cannot be described in terms of an ionization rate, as in perturbation theory.[14] In this context the peak width is roughly connected to the laser bandwidth $\Delta\omega$ ($\Delta\omega=2\pi/T$), we see in Fig. 3 that the peak structures broaden when the pulse duration decreases. It is worth to mention that the breakdown threshold for CsI corresponds to $\sim5\times10^{13}$ W/cm^2, therefore we have not performed calculations above 10^{13} W/cm^2. In agreement with earlier estimations, for $I=0.5$–3.0×10^{12} W/cm^2, which are the intensities measured in the experiments,[1–4] one- and two- photon (and partly three-photon) transitions between the two lowest branches play a major role in electron heating. These transitions are followed by subsequent photon absorptions to upper branches in the spectrum.

We investigate now the effect of the crystal parameters (U_g and the lattice period a). On one hand, increasing U_g leads to the modification of the band structure, thus the one-(multi-) photon resonances between bands shift their position in k space. On the other hand the dipole matrix elements increase as well. It is well known that, in terms of nearly free electron model,[15] one has to distinguish between regions of nondegenerated dispersion curves (regions 1) and the regions of intersection of these curves (regions 2). In regions 1 the points correspond to arbitrary values of k which are located far from the points of the intersection of energy dispersion curves. In the model of free electrons the energy difference $\Delta E_{0,k}^{G'G}=|E_{0,k}^{G'}-E_{0,k}^{G}|$ between two branches of free electron dispersion curves $E_{0,k}^{G}=\hbar^2(k-G)^2/2m$ is greater than $|U_{G-G'}|$, U_G being the Fourier transformation of the potential energy [see Eq. (2.2) and below] and $G=2\pi n/a$. The energy shift at the points of the first type is proportional to $|U_{G-G'}|^2/\Delta E_{0,k}^{G'G}$ (second order of the perturbation theory), whereas the dipole matrix elements are proportional to $|U_{G-G'}|$. The energy shift in region 2 is proportional to $|U_{G-G'}|$ (perturbation theory in degenerated case), whereas matrix elements are saturated and do not depend on $|U_{G-G'}|\sim U_g$. Note that the width of region 2 in k space is proportional to U_g. Therefore the trend in both regions results in the increase of the mean probability of interbranch transitions in the conduction band with the increase of U_g.

Increasing the lattice period a without changing of U_g (in terms of Kronig-Penny model this means that the b/a ratio and U_0 remain unchanged) leads to a significant decrease of the gap between two branches (but the gap at the edge of the first Brillouin zone remains unchanged), thus, the one—(multi-) photon resonances (see Fig. 1) shift towards Γ point. Besides, the maximal order of primary peaks

$$n_{\max}=\mathrm{int}\left[\frac{\max(\Delta E_{21})}{\hbar\omega}\right]$$

decreases (ΔE_{12} is the energy gap between branches 1 and 2 at Γ point). Therefore, electron heating should be more effective in crystals with higher values of the lattice constant a because one- and two-photon transitions should be more effective near the bottom of the conduction band, where the concentration of electrons is expected to be large after the initial ionization stage.

IV. RESOLUTION OF THE TDSE IN THREE-DIMENSIONS

As noticed above, the one-dimensional model underestimates the efficiency of electron heating since the density of states in the conduction band has not the proper behavior. We have performed 3D calculations for the case of the excitation of a crystal with parameters corresponding to CsI by femtosecond Ti: Sapphire laser pulses at peak intensities of $1-10$ TW/cm^2 and different pulse duration with polarization along [001] direction. In our simulation we assumed that initially (i.e., after the first ionization stage from defects) all electrons are located on the lowest branch of the dispersion curve of the conduction band. The transition probability to upper levels is obtained by solving the TDSE in three dimensions. We used the number of plane waves $N_{\max}=23$ in Eq. (2.3), we have verified that the results are unchanged when this number is increased. The probabilities, versus the initial electron energy, are presented in Fig. 4. Calculations are performed for various U_g (top panel), pulse durations T (middle panel), and intensities (bottom panel). We clearly see that, in all cases, the transition probability to the upper bands depends dramatically on the initial electron energy. Our findings are consistent with TDSE calculations performed in 1D but, in general the structures are more pronounced in the 3D case because, at contrast with the 1D case, there are multiple points corresponding to each resonance. The two upper panels show that, overall, the order of magnitude of the transition probability does not dramatically depend on U_g and T. The role of the pulse duration is twofold. On the one hand, the enlargement of T increases the interaction time. On the other hand, the radiation spectrum becomes narrower and therefore the fraction of "favorable to heating" points in the Brillouin zone decreases. The role of the variation of U_g is more straightforward, since in frames of perturbation theory transition matrix elements are proportional to U_g, therefore the heating is weaker for small U_g. The bottom panel shows

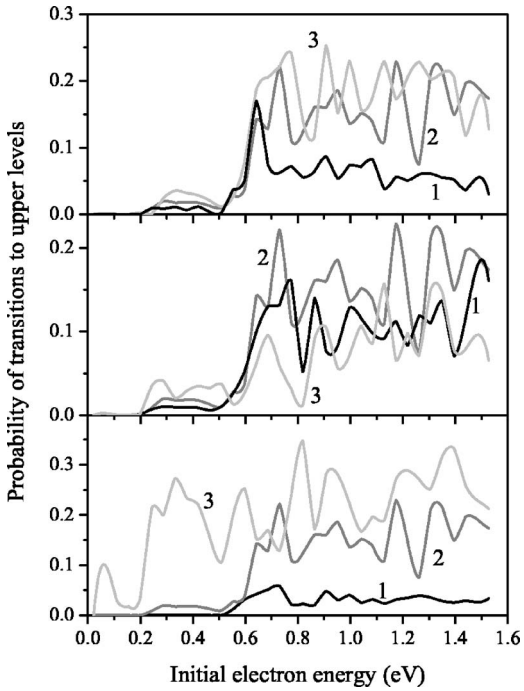

FIG. 4. Dependence of the transition probability to the upper bands (probability of escape) for an electron, initially located on the lowest band, after the interaction with the laser pulse. Top panel: Influence of U_g: U_g equals to one half of U_g corresponding to CsI crystal (1), U_g corresponds to CsI crystal (2), and twice of this U_g (3); intensity of 3 TW/cm^2, pulse duration is of 40 fs; Middle panel: Influence on pulse duration: 20 fs (1), 40 fs (2), and 80 fs (3); intensity of 3 TW/cm^2, U_g corresponds to CsI crystal; Bottom panel: Influence on pulse intensity: intensities of 1 TW/cm^2 (1), 3 TW/cm^2 (2) and 10 TW/cm^2 (3); pulse duration is 40 fs and U_g corresponds to CsI crystal. For all curves the photon energy is 1.55 eV and the lattice constant corresponds to CsI crystal.

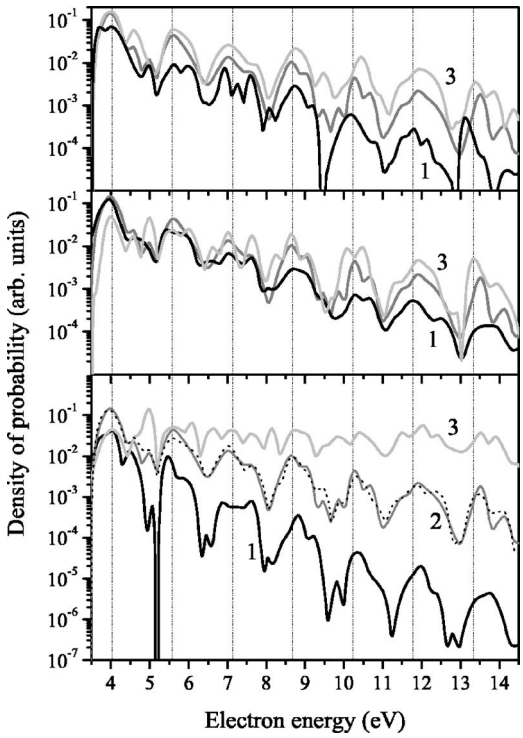

FIG. 5. Spectra of electrons in the conduction band after interaction with laser pulse. Top panel: Influence of U_g: U_g equals to one half of U_g corresponding to CsI crystal (1), U_g corresponds to CsI crystal (2), and twice of this U_g (3); intensity of 3 TW/cm^2, pulse duration is of 40 fs; Middle panel: Influence on pulse duration: 20 fs (1), 40 fs (2), and 80 fs (3); intensity of 3 TW/cm^2, U_g corresponds to CsI crystal; Bottom panel: Influence on pulse intensity: intensities of 1 TW/cm^2 (1), 3 TW/cm^2 (2) and 10 TW/cm^2 (3); pulse duration is 40 fs and U_g corresponds to CsI crystal. For all curves the photon energy is 1.55 eV and the lattice constant correspond to CsI crystal. Dotted and solid curves (2) correspond to calculations with different numbers of sampling points (doubled number in the case of dotted line). Vertical grid has step equal to photon energy (1.55 eV).

that there is an energy threshold for direct transitions from the lowest branch, i.e., electrons having a lower energy than a minimum required do not leave the lowest branch. As expected, the value of this threshold decreases as the peak laser intensity increases. For laser intensity of 10 TW/cm^2 it lies near the energy zero (i.e., near Γ point) while, at 1 TW/cm^2, it is about 0.6 eV. Therefore, at low intensity, the heating process, to be efficient, requires that the initial ionization process populates the lower branch above the mentioned minimum energy.

The electron spectrum in the conduction band of CsI, after interaction with the laser pulse, is presented in Fig. 5. As in Fig. 4 we show the influence of U_g, T, and I, the laser intensity (bottom panel). Here we assumed that the initial distribution of electrons is uniform from the bottom of the conduction band up to the photon energy $\hbar\omega$ and zero for higher energies. Such a model for the initial distribution is based on the hypothesis that the initial ionization process is dominated by a one-photon absorption from defects. Therefore $\hbar\omega$ is an upper limit for the energy of electrons in the lower conduction band. We take into account neither the energy distribution of defect levels nor the density of electron states near the bottom of the conduction band. As in Fig. 4, the upper panels show that the overall behavior of the electron spectrum is not strongly influenced by U_g and T. The role of these parameters is discussed above. The role of pulse duration is more evident from these spectra. For 80 fs pulses the resonant features in electron spectra become more prominent. The peak at 4 eV is lower for 80 fs since the increasing pulse duration allows cascade photon absorption with transition of electrons to states with higher energies. The bottom panel clearly shows the plateau structure at the higher intensity. The spectra calculated at lower intensities (1 and 3 TW/cm^2) clearly exhibit the characteristics of the perturbative regime with (i) peaks associated to the absorption of photons and (ii) with a linear decrease of the density of probability (in logarithm scale). The structure of the electron spectra results mainly from resonant transitions, Rabi oscillations and nonperturbative effects. The role of numerical noise is low [the dotted curve (2) in the bottom panel of Fig. 5 shows a calculation resulting from doubling the number of sampling points within the Brillouin zone]. The first peak in the electron spectrum, just above 2.5 eV, corresponds to the electron spectrum resulting from one-photon absorption. Figure 5 does not show the population of the lowest branch, corresponding to energies less than 1.5 eV. The sharp minimum at about 3.5 eV in the electron spectrum is connected with initial distribution of electrons when only a definite part of the Brillouin zone (with energies from 0 to $\hbar\omega$) is populated. Figure 4 shows that for low laser intensities electrons from 0 to 0.5 eV are not heated by the laser field. Due to momentum conservation the energies corresponding to one- and two-photon absorption from this latter region cannot be observed in the spectrum. At higher intensities Stark shift in the alternate field can partially remove this restriction. As the intensity increases, the plateau becomes flatter and its width also increases. These findings are in qualitative agreement with the observed spectra.[1–4]

V. CONCLUSIONS

We have investigated the irradiation of wide band-gap insulators with a femtosecond Ti:Sapphire laser pulse by using a quantum mechanical approach based on the resolution of the TDSE. We used a spectral method with a basis set of one-electron Bloch functions, calculated in a pseudopotential approximation. This approach greatly improves the precedent models where equidistant levels where used.[2,3,7,8] A one-dimensional model shows that the electron transfer from the lower conduction band to the higher one is already effective at intensity of 3×10^{12} W/cm^2. The model also shows that the perturbation theory is not valid at this intensity since ac Stark shifts and Rabi oscillations influence the photoexcitation. The three-dimensional model confirms these findings; the transfer of electrons to higher levels in the conduction band is even more effective since the density of states in the conduction band increases with energy in the 3D

case whereas it decreases in the 1D case. Regarding the electron spectrum, we have reproduced the wide plateau observed in the experiments at intensities of few terawatts per square centimeter. In order to explain the cutoff of the experimental spectrum we plan to include inelastic scattering due to electron-electron interactions in our treatment.

ACKNOWLEDGMENTS

B.N.Y. acknowledges the support of a NATO research grant and would like to thank R. Gayet for fruitful discussions. A.N.V. is grateful for the hospitality of CELIA, Université de Bordeaux I and acknowledges the support of Russian NSh 1771.2003.2 grant.

*Corresponding author. Electronic address: anv@ibrae.ac.ru

[1] A. N. Belsky, H. Bachau, J. Gaudin, G. Geoffroy, S. Guizard, P. Martin, G. Petite, A. Philippov, A. N. Vasil'ev, and A. N. Yatsenko, Appl. Phys. B **78**, 989 (2004).

[2] A. Belsky, P. Martin, H. Bachau, A. N. Vasil'ev, B. Yatsenko, S. Guizard, G. Geoffroy, and G. Petite, Europhys. Lett. **67**, 301 (2004).

[3] A. Belsky, A. Vasil'ev, B. Yatsenko, H. Bachau, P. Martin, G. Geoffroy, and S. Guizard, J. Phys. (Paris), Colloq. **108**, 113 (2003).

[4] B. N. Yatsenko, H. Bachau, A. N. Belsky, J. Gaudin, G. Geoffroy, S. Guizard, P. Martin, G. Petite, A. Philippov, and A. N. Vasil'ev, Phys. Status Solidi C **2**, 240 (2005).

[5] G. G. Paulus, W. Becker, W. Nicklich, and H. Walter, J. Phys. B **27**, L703 (1994).

[6] D. I. Vaisburd, P. A. Pal'yanov, and B. N. Semin, J. Appl. Spectrosc. **62**, 130 (1995).

[7] A. N. Belsky, A. N. Vasil'ev, and B. N. Yatsenko, Vestn. Mosk. Univ., Fiz., Astron. **2**, 38 (2003).

[8] B. Rethfeld, Phys. Rev. Lett. **92**, 187401 (2004).

[9] L. Plaja and L. Roso-Franco, Phys. Rev. B **45**, 8334 (1992).

[10] N. W. Ashcroft and N. D. Mermin, *Solid State Physics* (Holt, Rinehart and Winston, New York, 1976).

[11] M. L. Cohen and T. K. Bergstresser, Phys. Rev. **141**, 789 (1966).

[12] B. J. Austin, V. Heine, and L. J. Sham, Phys. Rev. **127**, 276 (1962).

[13] J. R. Chelikowsky and M. L. Cohen, Phys. Rev. B **14**, 556 (1976).

[14] L. D. Landau and E. M. Lifschitz, *Quantum Mechanics. Nonrelativistic Theory* (Pergamon, Oxford, New York, 1977).

[15] C. Kittel, *Introduction to Solid State Physics*, 7th ed. (John Wiley & Sons, New York, 1966).